Space-separated quantum cutting with silicon nanocrystals for photovoltaic applications

D. TIMMERMAN[1]*, I. IZEDDIN[1], P. STALLINGA[1,2], I. N. YASSIEVICH[3] AND T. GREGORKIEWICZ[1]

[1]Van der Waals–Zeeman Institute, University of Amsterdam, Valckenierstraat 65, NL-1018 XE Amsterdam, The Netherlands
[2]Center for Electronics, Opto-electronics and Telecommunications, University of The Algarve, Faro, Portugal
[3]A. F. Ioffe Physico-Technical Institute, RAS, St Petersburg, Russia
*e-mail: dtimmerm@science.uva.nl

Published online: 20 January 2008; doi:10.1038/nphoton.2007.279

For optimal energy conversion in photovoltaic devices (electricity to and from light) one important requirement is that the full energy of the photons is used. However, in solar cells, a single electron–hole pair of specific energy is generated when the incoming photon energy is above a certain threshold, with the excess energy being lost to heat. In the so-called quantum-cutting process, a high-energy photon can be divided into two, or more, photons of lower energy. Such manipulation of photon quantum size can then very effectively increase the overall efficiency of a device. In the current work, we demonstrate (space-separated) photon cutting by silicon nanocrystals, in which nearby Er^{3+} ions and neighbouring nanocrystals are used to detect this effect.

One of the major problems in photovoltaic devices is the large range of wavelengths over which energy conversion has to take place. As an example, a solar cell must work well in the visible range, where most of the energy is available, but should also be able to convert the UV and infrared (IR) parts of the spectrum, which nevertheless contain a substantial fraction of the solar energy. Effective harvesting of energy from UV and IR photons is a necessary condition for improving the efficiency of solar cells and to reduce the cost per watt. On the lower energy side, conversion is limited by the bandgap, E_g, below which photon absorption is not possible. On the other side of the spectrum, for high-energy photons, a substantial part of the incoming photon energy $h\nu$ is often wasted in the conversion, as the energy excess represented by $h\nu - E_g$ is transformed into kinetic energy of the electron–hole pair, and subsequently converted to heat. Thus, a bandgap-optimized p–n junction ('first generation') solar cell is a 'one-electron–hole-pair-for-one-photon device', with an efficiency limited to ~30%—the Shockley–Queisser limit[1]—for a bandgap of 1.1 eV, close to that of silicon. Even modern (organic) materials[2,3] and device designs, such as thin-film devices[4] ('second generation'), or Grätzel cells of blended hole-transporting and electron-transporting materials[5] ('third generation'), cannot avoid this theoretical limit. Stacked layers (tandem devices, 'fourth generation') with the bandgap of each layer optimized for a specific wavelength can increase the efficiency, but also increase the complexity and cost of the device.

A similar situation arises in light-emitting devices. Ideally, these should generate photons only in the visible range, but existing devices often emit in a much wider spectrum (for example, fluorescent lamps). By using fluorescence, the energy of the emitted UV photons can be reduced to the visible range, but in this case, in the 'one-photon-for-one-photon' down-conversion, a large part of the photon energy is lost.

For photovoltaic applications it is therefore very important to develop a scheme that allows the use of the excess energy that would otherwise be wasted in conversion. An elegant solution is to use quantum cutting. This process involves the transformation of a high-energy photon into two (or more) photons of lower energy, hence 'cutting' the energy quantum. Ideally, the down-converted photons are in a suitable range of the spectrum and can be further used without loss of energy. Such quantum cutting has been demonstrated in rare-earth systems[6] and been applied in fluorescent tubes. A similar idea involves the generation of multiple electron–hole pairs by a single high-energy photon absorbed in a nanocrystal (NC). This process, termed multiple exciton generation (MEG) or carrier multiplication (CM), has been observed in NCs made from different semiconductor materials[7–12], including generation of a remarkable seven excitons for a single incoming photon[13]. Recently, the same phenomenon has also been demonstrated in colloidal silicon NCs (ref. 14). The lifetimes of multiexcitons in an NC were found to be very short (50–100 ps and shorter, depending on the material and NC size[15]) owing to the enhanced Auger recombination and subsequent fast carrier cooling[16]. Therefore, harvesting of this energy—by means of carrier extraction or light generation—is difficult, as only the 'last' exciton has a relatively long lifetime and is usable.

In the present work we report on the observation of quantum cutting in NCs of silicon, still the most popular material for electronic and photovoltaic applications, embedded in a SiO_2 matrix. We show that in the quantum-cutting process, energy can be transmitted to outside the photoexcited system. In the pilot experiment, we used Er^{3+} ions outside the NCs as receptors for the down-converted energy, using their characteristic photoluminescence (PL) for detection of the phenomenon. Subsequently, we have demonstrated that a similar space-separated quantum cutting (SSQC) process takes place between the silicon NCs.

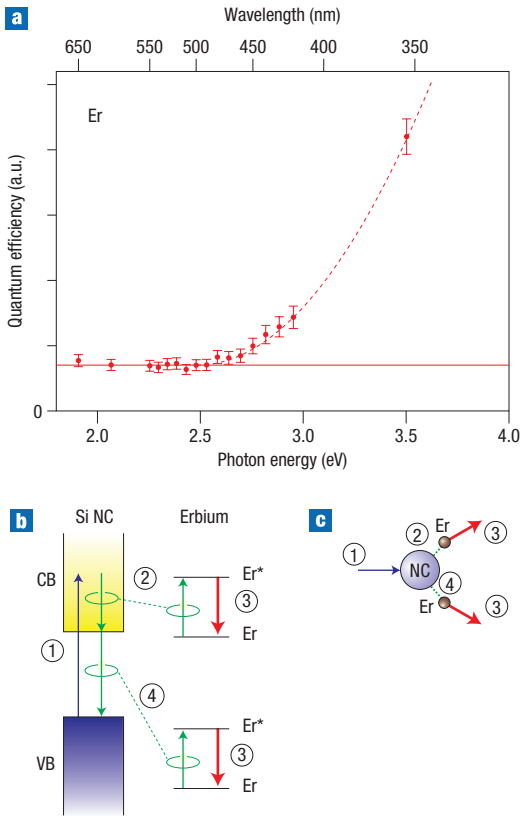

Figure 1 Space-separated quantum cutting in an erbium–silicon NC system. a, Relative quantum efficiency of erbium-related PL (1,535 nm) as a function of excitation energy. The quantum efficiency is determined here as the ratio of the (effective) excitation cross-section of erbium PL and the absorbed fraction of incident photons, at a particular wavelength. For each data point the absorbed photon fraction was measured and the excitation cross-section was determined from the plot of PL intensity versus excitation photon flux. As can be seen, the quantum efficiency is constant up to a certain photon energy. This indicates a single-photon process: one photon in, one photon out. The relation deviates from constant for the excitation energy at which the SSQC process sets in, where there arises the possibility of emission of two photons per one absorbed photon. In this case, the energy of the incoming photon is divided by the NC over two nearby Er^{3+} ions. The solid line represents a fit to the data points, whereas the dashed line at higher energies is only a guide to the eye. The error bars reflect the uncertainty in the value of the power of the laser, 10% for OPO and 15% for UV lasers, expressed as the standard deviation determined separately. **b**, Schematic of the SSQC process: 1, Excitation of the silicon NC with a high-energy photon transferring an electron from the valence band (VB) to the conduction band (CB) creating a hot electron–hole pair with excess energy; 2, intraband Auger process exciting an Er^{3+} ion and removing the excess energy; 3, erbium-related PL; and 4, excitation of a second Er^{3+} ion by conventional interband Auger process. **c**, Schematic illustrating the SSQC process with excitation of two nearby Er^{3+} ions.

The experiments were conducted on 2-μm-thick films of silicon NCs embedded in a SiO_2 matrix produced by sputtering on a quartz substrate[17]. The silicon NCs had an average diameter of 3.1 nm with a size dispersion of 14% and a density of approximately $4.1 \times 10^{18}\,cm^{-3}$. The average distance between the surfaces of adjacent NCs was ~3 nm, that is, comparable to the NC diameter. Some of the layers were erbium-doped during sputtering to a concentration of $2.8 \times 10^{19}\,cm^{-3}$. In this case, assuming a random distribution of both Er^{3+} ions and silicon NCs in the SiO_2 matrix, ~6.6% of the dopants should be contained inside the NCs and the rest dispersed in the SiO_2 (see Supplementary Information, Fig. S1, for the NC–erbium dopant distribution). The PL experiments were performed under pulsed excitation, provided in the visible range by a tunable optical parametric oscillator (OPO) pumped by a Nd:YAG laser (5 ns pulsewidth, 10 Hz repetition rate, 1–10 mJ per pulse), and in the UV range by the third harmonic of a Nd:YAG or dye laser pumped by a XeCl (308 nm) excimer laser. The wavelength of the PL was selected with a monochromator and detected with a Hamamatsu R5509-72 near-IR photomultiplier tube or a germanium photodiode (Edinburgh Instruments EI-A) connected to a digital oscilloscope where signal integration was carried out. The emerging emission was monitored at wavelengths of 1,535 nm and 914 nm for the erbium and NC-related PL, respectively. Signal integration was performed over the entire PL decay-time window (typically from between 1 ms and a few milliseconds for NC- and erbium-related PL, respectively); the recorded PL intensity value therefore predominantly reflects the contributions of relatively slow radiative processes. In particular, for the erbium-related emission, only the approximately millisecond component due to Er^{3+} ions in SiO_2 is accounted for, with the contribution from fast-decaying dopants[18] being negligible. A Varian Cary-50 UV-VIS spectrophotometer was used for absorption measurements in the visible and the UV regions. All measurements were performed at room temperature.

In the first experiment the erbium-related PL was monitored as a function of excitation wavelength and compared to the absorption of the sample at that wavelength. At the start of a cycle, the NC absorbs a photon and an electron–hole pair is created. On its recombination, one relaxation path will transfer the energy to a neighbouring Er^{3+} ion, placing it in an excited state. Subsequently, the Er^{3+} ion relaxes back to the ground state by emitting a long-wavelength (IR) photon, which can be detected as PL at 1,535 nm. This process implies that the erbium-related PL should be correlated to photon absorption by silicon NCs. (It should be mentioned that under the present experimental conditions no direct absorption by erbium takes place, and therefore any erbium-related emission must originate from photon absorption in silicon NCs). From this it follows that the total number of photons emitted (by erbium) should be correlated to the total number of photons absorbed (by silicon NCs). To describe this we introduce the PL quantum efficiency, which we define as the ratio of the number of photons coming out of the sample to the number of photons absorbed: $\eta = N_{PL}/N_{abs}$. Because, in our set-up, the luminescence intensity is not calibrated and its absolute value cannot be measured, we cannot determine the absolute values of this efficiency. Nevertheless, the relative efficiency enables direct comparison of the different mechanisms leading to emission, in the same system investigated and in the same set-up, as reported here. Fig. 1a shows the experimentally measured quantum efficiency of erbium PL. Each data point in this figure represents the ratio of the PL excitation cross-section to the fraction of absorbed photons for a particular wavelength of the incoming light (see Supplementary Information for a detailed derivation of the relative quantum efficiency). In each case, the PL excitation cross-section was determined from the slope of the plot of PL intensity versus laser photon flux in the linear region. In this way, the effective excitation cross-section of erbium emission at different wavelengths can be compared, and it is this that is most relevant for the experiment. The wavelength dependence of the fraction of the incident light that is absorbed by the sample is measured in a separate experiment.

For a single-photon generation process, the correlation between the number of absorbed and emitted photons is linear and the ratio constant: with a certain efficiency a long-wavelength photon is emitted by the Er^{3+} ion for every short-wavelength photon absorbed by the silicon NC. From Fig. 1a it is evident that this scenario is indeed followed for the lower range of excitation energies. However, a clear enhancement is seen for energies above a certain threshold, ~2.6 eV (480 nm). At this energy, the quantum efficiency of the energy transfer to erbium increases, as double-photon generation kicks in at this point. The process is schematically illustrated in Fig. 1b; the excess energy ΔE of the 'hot' carrier ($\Delta E = h\nu - E_{NC}$, where $h\nu$ and E_{NC} are photon and exciton energies, respectively) is large enough to allow for an Auger process of intraband relaxation with simultaneous erbium excitation[18]. As a result, two Er^{3+} ions can be excited per single photon absorbed by the NC, with the second resulting from a conventional band-to-band Auger process, as indicated in the schematic. Analysing the energy diagram in Fig. 1b, such a process is expected for photon energies exceeding the sum of the silicon NC bandgap (~1.5 eV) and the erbium excitation (0.8 eV), thus above ~2.3 eV. Note that the decay time and also the saturation level of erbium-related PL are identical for below- and above-threshold pumping (see Supplementary Information, Figs S2 and S3).

Although the above-described experiment concerns erbium excitation by silicon NCs, it illustrates the SSQC process, with an Er^{3+} ion serving as a receptor[19] of the down-sized energy quanta. In a similar way, part of the energy can be transferred to create an exciton in a neighbouring NC by converting a high-energy (UV) photon absorbed in one of them. There is only one condition: these NCs must be located within the energy transfer range[18]. To demonstrate this process, we repeated the same experiment for a sample without erbium doping, correlating the silicon NC-related exciton PL, monitored at 914 nm, with the absorbed photon fraction. The results are illustrated in Fig. 2. Again, a constant ratio is observed, which, in this case, extends to a larger energy range. This was anticipated, as double-photon generation is expected only for photons with quantum energy at least twice that of the NC bandgap, $h\nu > 2E_{NC} \approx 3$ eV. In full agreement with this expectation, we see that the data obtained in the UV range fall clearly outside the dependence determined for low-energy excitation. This result demonstrates that the NCs themselves can also be the receiving elements in the SSQC process, albeit at higher energies; in other words, a second silicon NC can be excited by a neighbouring silicon NC containing a hot electron–hole pair. The partly de-excited first silicon NC will still produce PL owing to the 'cold' electron–hole pair (exciton). Thus, when the energy of the incident photon exceeds a certain threshold, relaxation back to the ground state can occur through emission of two photons in the silicon NC exciton PL wavelength range.

We will now comment on a possible physical mechanism behind the SSQC phenomenon. As pointed out previously, the SSQC bears close resemblance to the MEG process in which two, or more, electron–hole pairs are induced in one NC on absorption of a single photon. The microscopic origin of MEG is under debate and several possibilities have been suggested:

(1) Impact ionization by a hot carrier created as the result of the photon absorption[9,10].
(2) Coherent superposition of single and multiexciton states[20] due to the strong Coulomb interaction of carriers confined in NCs, which should take place when the energy relaxation rate of a single electron–hole pair is lower than both the two-exciton state thermalization rate and the rate of Coulomb coupling between single- and two-exciton states.

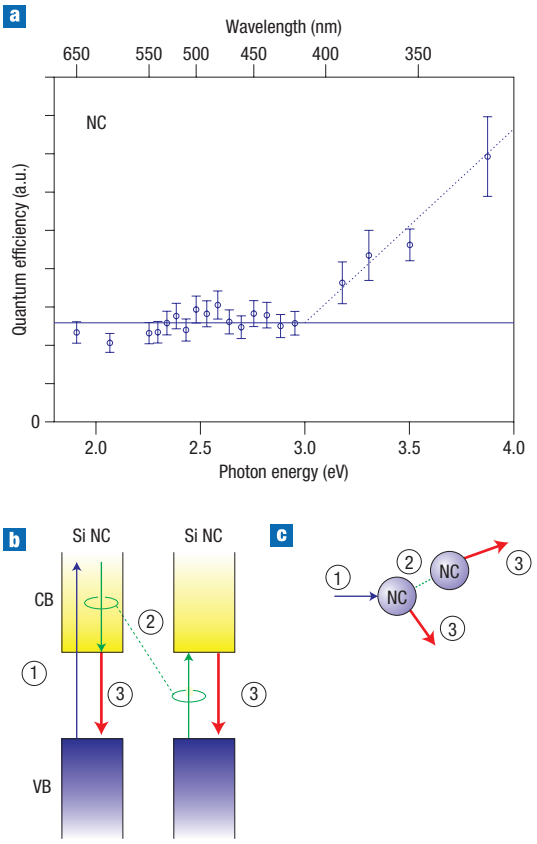

Figure 2 Space-separated quantum cutting between silicon NCs. Results for an erbium-free solid-state dispersion of silicon NCs in a SiO_2 matrix. **a**, Quantum efficiency of the NC-related PL (detected at 914 nm) as a function of excitation energy, illustrating that (neighbouring) NCs can themselves also be the energy-receiving systems. Quantum cutting appears now at a larger energy than the incoming photon because the bandgap of silicon NCs is larger than the erbium excitation energy, and a larger UV photon excess energy ($h\nu - E_{NC}$) is thus needed. **b**, Diagram of the processes involved: 1, excitation of the silicon NC with a high-energy photon creating a hot electron–hole pair with excess energy; 2, intraband Auger process exciting a neighbouring NC, removing the excess energy; 3, NC exciton luminescence. **c**, Schematic of the process, showing one photon absorbed by one NC, and two photons emitted by distinct NCs.

(3) Multiexciton formation through a virtual state[21,22]. This process can be described by second-order perturbation theory, and two possible scenarios, with comparable rates, have been proposed. The first proceeds through a virtual single-exciton state. In this case, the direct optical transition from vacuum to a single-exciton state is followed by a transition into the final two-exciton state owing to Coulomb interaction[21]. In the second channel, the first step is the transition initiated by the Coulomb interaction from vacuum to a two-exciton state, and the second step is an optical intraband transition[22].

Processes 1 and 2 can be responsible for MEG without any delay, that is, the instant a photon is absorbed, and can be effective for the production of multiple excitons in a single NC. However, extra excitons occurring in the same NC recombine on a picosecond timescale[15].

The impact ionization process (1) starts with some delay after the absorption. It proceeds through a real state, when the hot

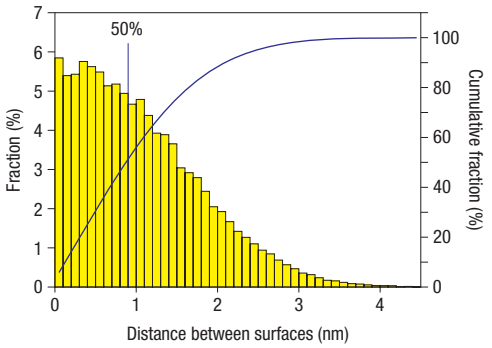

Figure 3 Nearest-neighbour distance distribution. A simulation of the distribution of nearest neighbours for the solid-state dispersion of silicon NCs in a SiO_2 matrix (erbium-free) investigated in this study. More than 50% of the NCs have a nearest neighbour within 1 nm of their surface.

electron–hole pair is created by the absorbed photon with energy exceeding the energy gap. This process is well known for bulk semiconductors, where it increases the number of photoexcited excitons by less than ~1%. It may be expected that the impact ionization rate should rise dramatically in the case of NCs owing to the strong Coulomb interaction of confined carriers and the decreasing rate of phonon emission caused by the discrete spectrum[9,10]. Indeed, pseudopotential calculations predict a higher rate of impact ionization in CdSe dots than in bulk material for electrons with excess energies just above the bottom of the conduction band[23].

Our preliminary theoretical considerations indicate that impact ionization is the most suitable process to account for the SSQC phenomenon reported here. The effective dielectric constant governing the Coulomb interaction between carriers in different NCs embedded in the SiO_2 matrix is considerably smaller than the dielectric constant of silicon. Using the Auger recombination rate (the reverse process to impact ionization) inside the silicon NC calculated previously[24], we obtain a value of the order of between 10^{10} and $10^{11}\ s^{-1}$ for the rate of the process under consideration for two NCs at a distance of less than 1 nm. This rate is comparable to the energy relaxation rate determined by the Auger process between carriers confined in one silicon NC of 3 nm diameter when there is one exciton per NC (ref. 25). From the NC–NC distance distribution depicted in Fig. 3, we conclude that more than 50% of all NCs have their closest neighbour at a distance of less than 1 nm from the surface, that is, sufficiently close to facilitate the proposed energy transfer. (It is worth mentioning that for direct-bandgap NCs faster cooling rates, of the order of $10^{12}\ s^{-1}$, are commonly reported.)

Note that the observed linear increase of SSQC quantum efficiency for photon energies higher than the threshold value, experimentally observed in this study for silicon NCs (Fig. 2) is in agreement with the calculated linear increase of the number of final states[26] and therefore supports the microscopic mechanism based on impact ionization. Yet additional support comes from measurements performed in a sample with a similar erbium concentration and NC size, but with a lower NC concentration, that is, with a larger erbium–NC separation. In this case the observed SSQC process shows a similar onset energy but lower quantum efficiency, providing an independent verification of the proposed mechanism.

For completeness, we recall that the Förster resonant energy transfer (FRET), which has been shown to be responsible for long-range energy diffusion in a closely packed CdSe quantum solid[27], has a low probability of occuring for silicon NCs owing to the indirect bandgap. It is nevertheless fair to mention that the final identification of the microscopic mechanism of the SSQC process (as well as that of MEG) will require further investigation. In particular, the kinetics of the process should be investigated by PL and induced absorption.

In summary, we have shown here how quantum cutting (one photon in, two photons out) can take place in systems based on silicon NCs. In contrast to the earlier work on multiexciton generation in semiconductor NCs, the energy quanta down-converted in the SSQC process are transferred to external objects—Er^{3+} ions and neighbouring NCs—from where they can be emitted in the form of photons, or harvested in a different manner. In this way, true space-separated photon cutting takes place. The demonstration of the SSQC process for silicon is technologically interesting in view of the prominent role of silicon and silicon-derived materials in electronic, optoelectronic and especially photovoltaic applications. Moreover, the use of NCs provides the additional appealing feature that the energy levels can be tuned to suit the application by changing the size of the particles[28,29]. Also, the efficiency of the SSQC process can be adjusted by changing the separation between individual NCs. The ideas and results presented here may lead the way to a substantial improvement in photovoltaic devices, both solar cells and light-emitting elements. For solar cells it has been shown theoretically that multiple exciton generation[30] and photon down-conversion[31] can increase the efficiency beyond the Shockley–Queisser limit. Interestingly, the indirect nature of the silicon bandgap, which is preserved in silicon NCs, and which is detrimental to photonic applications, turns out to be beneficial here, as the relatively long exciton lifetime (in comparison with direct-bandgap NCs) simplifies energy extraction for photovoltaic applications.

Received 13 August 2007; accepted 28 November 2007;
published 20 January 2008.

References

1. Shockley, W. & Queisser, H. J. Detailed balance limit of efficiency of *p–n* junction solar cells. *J. Appl. Phys.* **32,** 510–519 (1961).
2. Huynh, W. U., Dittmer, J. J. & Alivisatos, A. P. Hybrid nanorod–polymer solar cells. *Science* **295,** 2425–2427 (2002).
3. Peumans, P., Uchida, S. & Forrest, S. R. Efficient bulk heterojunction photovoltaic cells using small-molecular-weight organic thin films. *Nature* **425,** 158–162 (2003).
4. O'Regan, B. & Grätzel, M. A low-cost, high-efficiency solar cell based on dye-sensitized colloidal TiO_2 films. *Nature* **353,** 737–740 (1991).
5. Shah, A., Torres, P., Tscharner, R., Wyrsch, N. & Keppner, H. Photovoltaic technology: The case for thin-film solar cells. *Science* **285,** 692–698 (1999).
6. Wegh, R. T., Donker, H., Oskam, K. D. & Meijerink, A. Visible quantum cutting in $LiGdF_4$:Eu^{3+} through downconversion. *Science* **283,** 663–666 (1999).
7. Luque, A., Martí, A. & Nozik, A. J. Solar cells based on quantum dots: Multiple exciton generation in films of electronically coupled PbSe quantum dots. *MRS Bull.* **32,** 236–241 (2007).
8. Nozik, A. J. Quantum dot solar cells. *Physica E* **14,** 115–120 (2002).
9. Schaller, R. D. & Klimov, V. I. High efficiency carrier multiplication in PbSe nanocrystals: implications for solar energy conversion. *Phys. Rev. Lett.* **92,** 186601 (2004).
10. Ellingson, R. J. *et al.* Highly efficient multiple exciton generation in colloidal PbSe and PbS quantum dots. *Nano Lett.* **5,** 865–871 (2005).
11. Schaller, R. D., Petruska, M. A. & Klimov, V. I. Effect of electronic structure on carrier multiplication efficiency: Comparative study of PbSe and CdSe nanocrystals. *Appl. Phys. Lett.* **87,** 253102 (2005).
12. Murphy, J. E. *et al.* PbTe colloidal nanocrystals: synthesis, characterization, and multiple exciton generation. *J. Am. Chem. Soc.* **128,** 3241–3247 (2006).
13. Schaller, R. D., Sykora, M., Pietryga, J. M. & Klimov, V. I. Seven excitons at a cost of one: Redefining the limits for conversion efficiency of photons into charge carriers. *Nano Lett.* **6,** 424–429 (2006).
14. Beard, M. C. *et al.* Multiple exciton generation in colloidal silicon nanocrystals. *Nano Lett.* **7,** 2506–2512 (2007).
15. Klimov, V. I., Mikhailovsky, A. A., McBranch, D. W., Leatherdale, C. A. & Bawendi, M. G. Quantization of multiparticle Auger rates in semiconductor quantum dots. *Science* **287,** 1011–1013 (2000).
16. Hendry, E. *et al.* Direct observation of electron-to-hole energy transfer in CdSe quantum dots. *Phys. Rev. Lett.* **96,** 057408 (2006).
17. Fujii, M., Yoshida, M., Kanzawa, Y., Hayashi, S. & Yamamoto, K. 1.54 μm photoluminescence of Er^{3+} doped into SiO_2 films containing Si nanocrystals: Evidence for energy transfer from Si nanocrystals to Er^{3+}. *Appl. Phys. Lett.* **71,** 1198–1200 (1997).
18. Izeddin, I., Moskalenko, A. S., Yassievich, I. N., Fujii, M. & Gregorkiewicz, T. Nanosecond dynamics of the near-infrared photoluminescence of Er-doped SiO_2 sensitized with Si nanocrystals. *Phys. Rev. Lett.* **97,** 207401 (2006).

19. Polman, A. Erbium as a probe of everything? *Physica B* **300,** 78–90 (2001).
20. Shabaev, A., Efros, A. L. & Nozik, A. J. Multiexciton generation by a single photon in nanocrystals. *Nano Lett.* **6,** 2856–2863 (2006).
21. Schaller, R. D., Agranovich, V. M. & Klimov V. I. High-efficiency carrier multiplication through direct photogeneration of multi-excitons via virtual single-exciton states. *Nature Phys.* **1,** 189–194 (2005).
22. Rupasov, V. I. & Klimov, V. I. Carrier multiplication in semiconductor nanocrystals via intraband optical transitions involving virtual biexciton states. *Phys. Rev. B* **76,** 125321 (2007).
23. Califano, M., Zunger, A. & Franceschetti, A. Direct carrier multiplication due to inverse Auger scattering in CdSe quantum dots. *Appl. Phys. Lett.* **84,** 2409–2411 (2004).
24. Mihalcescu, I. *et al*. Saturation and voltage quenching of porous-silicon luminescence and the importance of the Auger effect. *Phys. Rev. B* **51,** 17605–17613 (1995).
25. Trojanek, F., Neudert, K., Brittner, M. & Maly, P. Picosecond photoluminescence and transient absorption in silicon nanocrystals. *Phys. Rev. B* **72,** 075365 (2005).
26. Allan, G. & Delerue, C. Role of impact ionization in multiple exciton generation in PbSe nanocrystals. *Phys. Rev. B* **73,** 205423 (2006).
27. Kagan, C. R., Murray, C. B. & Bawendi, M. G. Long-range resonance transfer of electronic excitations in close-packed CdSe quantum-dot solids. *Phys. Rev. B* **54,** 8633–8643 (1996).
28. Nanda, K. K., Kruis, F. E. & Fissan, H. Energy levels in embedded semiconductor nanoparticles and nanowires. *Nano Lett.* **1,** 605–611 (2001).
29. Murray, C. B., Norris, D. J. & Bawendi, M. G. Synthesis and characterization of nearly monodisperse CdE (E = S, Se, Te) semiconductor nanocrystallites. *J. Am. Chem. Soc.* **115,** 8706–8715 (1993).
30. Hanna, M. C. & Nozik, A. J. Solar conversion efficiency of photovoltaic and photoelectrolysis cells with carrier multiplication absorbers. *J. Appl. Phys.* **100,** 074510 (2006).
31. Trupke, T., Green, M. A. and Würfel, P. Improving solar cell efficiencies by down-conversion of high-energy photons. *J. Appl. Phys.* **92,** 1668–1674 (2002).

Acknowledgements

The authors acknowledge the contribution of M. Fujii, Kobe University, for sample preparation and characterization, and R. Sprik, W.J. Buma and M. de Groot, University of Amsterdam, for absorption and dye laser PL measurements. P.S. acknowledges the financial support of Stichting voor Fundamenteel Onderzoek Materie (FOM) during his sabbatical at the Van der Waals–Zeeman Institute.
Correspondence and requests for materials should be addressed to D.T.
Supplementary information accompanies this paper on www.nature.com/naturephotonics.